Acta Crystallographica Section D
Biological Crystallography
ISSN 0907-4449

Crystallization and preliminary X-ray diffraction studies of monomeric isocitrate dehydrogenase by the MAD method using Mn atoms

Yoshiaki Yasutake, Seiya Watanabe, Min Yao, Yasuhiro Takada, Noriyuki Fukunaga and Isao Tanaka*

Division of Biological Sciences, Graduate School of Science, Hokkaido University, Sapporo 060-0810, Japan

Correspondence e-mail: tanaka@castor.sci.hokudai.ac.jp

Received 18 May 2001
Accepted 30 July 2001

NADP$^+$-dependent isocitrate dehydrogenase (E.C. 1.1.1.42; IDH) is an enzyme of the Krebs cycle and catalyzes the oxidative decarboxylation reaction from DL-isocitrate to α-ketoglutarate, with a concomitant reduction of the coenzyme NADP$^+$ to NADPH. Single crystals of monomeric IDH from *Azotobacter vinelandii* in complex with DL-isocitrate and Mn^{2+} were obtained by the hanging-drop vapour-diffusion method at room temperature. One crystal diffracted to a resolution of 2.9 Å and was found to belong to the orthorhombic system; the space group was determined to be $P2_12_12_1$, with unit-cell parameters a = 108.4, b = 121.7, c = 129.7 Å. The asymmetric unit contains two molecules of monomeric IDH, corresponding to a V_M value of 2.66 Å^3 Da^{-1}. The crystals were frozen in a capillary by a flash-cooling technique and MAD data were collected using Mn atoms as anomalous scatterers on beamline BL41XU at SPring-8, Japan. The positions of two Mn atoms binding to two independent IDH molecules were located from Bijvoet difference Patterson maps.

1. Introduction

The Krebs cycle is a common metabolic pathway to completely oxidize fuel molecules. Isocitrate dehydrogenase (IDH) catalyzes the oxidative decarboxylation step of DL-isocitrate to yield α-ketoglutarate and CO_2 in the Krebs cycle (Chen & Gadal, 1990). The α-ketoglutarate is known to be a key substance in biosyntheses of cell constituents *via* reductive amination to glutamate.

Most bacterial IDHs are NADP$^+$-dependent enzymes and form a dimeric structure with molecular weights of 40–50 kDa per subunit (Chen & Gadal, 1990). *Escherichia coli* IDH is one of the dimeric IDHs composed of two identical subunits and has been studied the most extensively. Analysis of the deduced amino-acid sequences of the adenine nucleotide-specific dehydrogenases has revealed that *E. coli* IDH is extremely unique because its lack of a Rossmann fold motif (Hurley *et al.*, 1989), which is the typical sequence for the recognition of coenzymes that has been conserved by many other dehydrogenases such as lactate dehydrogenase (Rossmann *et al.*, 1974). The crystal structure of *E. coli* IDH has already been determined and the structural details of substrate and coenzyme binding sites have been elucidated (Hurley *et al.*, 1989, 1991). Further structural studies of site-directed mutants showed the regulation mechanism of its enzymatic activity (Hurley *et al.*, 1990, 1996; Cherbavaz *et al.*, 2000).

In contrast to dimeric IDHs, monomeric IDHs with molecular weights of 80–100 kDa have been found in a few species of bacteria such as *Colwellia maris*, *Rhodomicrobium vannielii*, *Corynebacterium glutamicum* and *Azotobacter vinelandii* (Chen & Gadal, 1990). Recent success in cloning and sequencing the gene encoding monomeric IDH has allowed us to determine that the amino-acid sequences of monomeric and dimeric IDHs are completely different from one another (Ishii *et al.*, 1993). The enzymatic functions of these two types of IDH, however, are indistinguishable in *in vitro* and *in vivo* experiments (Chen & Gadal, 1990). These results suggest that these two types of IDH have evolved independently.

We have successfully purified and crystallized monomeric IDH from the nitrogen-fixing bacterium *A. vinelandii*. As the IDH crystals are grown in a solution containing Mn^{2+}, which is required for maximum activation of monomeric IDH, we applied a multiwavelength anomalous diffraction (MAD) method (Hendrickson, 1991) using Mn atoms as anomalous scatterers. Although a few structures have been determined using the anomalous signal of Fe atoms (K absorption edge: 1.743 Å), no structures have been reported based on the use of Mn atoms as anomalous scatterers. The wavelength of the Mn K edge is 1.896 Å, so that absorption of the X-rays and subsequent radiation damage of the crystal become a serious problem (Helliwell, 1992). Nonetheless, the anomalous difference Patterson maps clearly showed two Mn atoms

© 2001 International Union of Crystallography
Printed in Denmark – all rights reserved

in an asymmetric unit. Here, we report the crystallization and preliminary X-ray diffraction studies of monomeric IDH using Mn atoms as anomalous scatterers.

2. Materials and methods

2.1. Purification of monomeric IDH

A. vinelandii IAM1078 was cultured at 303 K with 50 h of vigorous shaking in Burk's N-free medium with modifications (pH 7.6). Cultured cells were harvested by centrifugation at 5 000 rev min^{-1} for 20 min, then washed two times with chilled 20 m*M* potassium phosphate buffer pH 6.8 containing 2 m*M* $MgCl_2$, 10%(*w*/*v*) glycerol and 10 m*M* 2-mercaptoethanol (referred to as buffer *A*). After the cells were disrupted sonically on ice, the supernatant of cell extracts was obtained by centrifugation at 18 000 rev min^{-1} for 20 min.

All purification procedures were performed at 277 K or below. The supernatant of the cell extract was diluted by buffer *A*. After processing with protamine sulfate, the supernatant of the cell extract was fractionated between 45 and 75% saturation of ammonium sulfate by adding solid ammonium sulfate. The precipitate was dissolved in a small volume of buffer *A* and the solution was dialyzed overnight against an excess of buffer *A* containing 1.3 *M* ammonium sulfate. The supernatant was applied to a phenyl-Sepharose CL-4B column, subjected to hydrophobic chromatography, equilibrated with the dialyzing buffer and then washed with the same buffer. Proteins were eluted using a reverse linear gradient of 1.3–0 *M* ammonium sulfate in buffer *A*. The fractions with high enzymatic activity were pooled, concentrated with polyethylene glycol (PEG) 20 000 and dialyzed against buffer *A*. The enzyme solution was loaded onto a column of DEAE-Toyopearl 650M, an anion exchanger, and equilibrated with buffer *A*. The enzyme was not absorbed onto the column and passed through during washing with buffer *A*. The recovered enzyme solution was concentrated, applied to a column of Red-Sepharose CL-6B and washed with buffer *A*. The column was then washed further with the same buffer containing 50 m*M* NaCl and the enzyme was specifically eluted with buffer *A* containing 4 m*M* DL-isocitrate (referred to as buffer *B*). The fractions containing the target protein were pooled and applied to a gel-filtration column of Sephadex G-100 with buffer *A*. Monomeric IDH was eluted as a single peak and the fractions containing high enzymatic activity were analyzed by SDS–PAGE to judge the purity of the preparation. Purified enzyme solution was concentrated to approximately 20 mg ml^{-1}, dialyzed against buffer *B* and frozen at 193 K until use.

2.2. Crystallization

All crystallization experiments were carried out by the hanging-drop vapour-diffusion method in a 24-well tissue-culture Linbro plate (ICN Inc.) at 291 or 277 K. Each drop was formed by mixing equal volumes (2–5 µl) of protein solution and the reservoir solution. The protein concentration was 12 mg ml^{-1} before mixing with the reservoir solution. The initial trial of crystallization was carried out using Hampton Research Crystal Screens I and II. After the initial crystallization trial using screening kits, we prepared a reservoir solution containing 4.0 m*M* $MnCl_2$ and 4.0 m*M* DL-isocitrate for further optimization of crystallization conditions such as pH, protein concentration, temperature, precipitants and additives.

2.3. MAD data collection and the processing procedure

As the crystals of *A. vinelandii* IDH were grown with Mn^{2+}, we decided to use the Mn atom as an anomalous scatterer for structure determination using the MAD method. The crystals were prepared in a solution containing 20%(*v*/*v*) glycerol so that they could be flash-cooled without soaking them in a cryoprotectant. The flash-cooled crystals prepared by the standard technique using a CryoLoop (Hampton Research) diffracted with extremely high mosaicity. Therefore, we attempted to freeze the crystals in different ways. The best MAD data were collected using a crystal mounted in a capillary over which a cold nitrogen stream was passed.

A MAD data set was collected from one crystal on beamline BL41XU at SPring-8. The crystal-to-detector distance was set to 120 mm (minimal distance on BL41XU) and the MAR-CCD detector was placed with an offset of 10.0 mm. Three wavelengths were selected for data collection based on the fluorescence spectrum of the Mn atom, corresponding to the maximum f'' (peak), the minimum f' (edge) and a reference wavelength (remote). The diffraction data were processed with *MOSFLM* (Leslie, 1993) and *SCALA* from the *CCP*4 suite (Collaborative Computational Project, Number 4, 1994).

3. Results and discussion

The first crystals were grown at 277 K under condition No. 46 of the Hampton Research Crystal Screen I (0.2 *M* calcium acetate, 0.1 *M* sodium cacodylate pH 6.5, 18.0%(*w*/*v*) PEG 8000). A dramatic improvement in the quality of IDH crystals was achieved in two trials in particular, one in which PEG 6000 was used as a precipitant and one in which glycerol was added to both the protein and reservoir solutions. After numerous other trials optimizing crystallization conditions

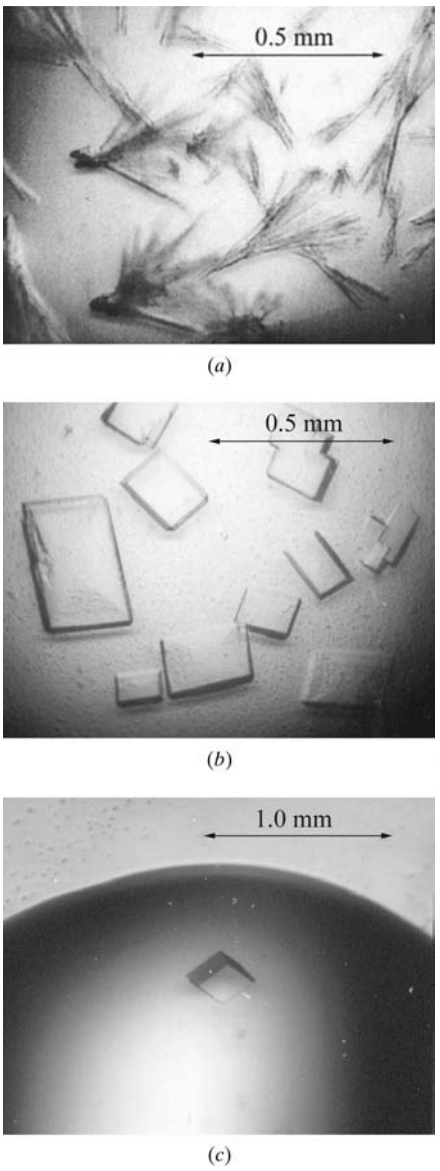

Figure 1
The improvement in the quality of monomeric IDH crystals. (*a*) Poor-quality crystals were initially obtained using the Hampton Research Crystal Screen I. (*b*) Better crystals were obtained using the Hampton Research Grid Screen PEG 6000. (*c*) The best crystal was obtained using the reservoir solution containing 20.0%(*v*/*v*) glycerol in six months. The size of the best crystal was approximately 0.3 × 0.3 × 0.2 mm.

Table 1
Data-collection statistics.

The values in parentheses refer to data in the highest resolution shell (3.06–2.90 Å).

	Peak	Edge	Remote
Beamline	BL41XU, SPring-8		
Space group	$P2_12_12_1$		
Unit-cell parameters (Å)	a = 108.4	a = 108.5	a = 108.4
	b = 121.6	b = 121.6	b = 121.7
	c = 129.7	c = 129.8	c = 129.7
Wavelength (Å)	1.8923	1.8934	1.8783
Resolution range (Å)	40.0–2.9 (3.06–2.90)		
No. of observed reflections	333859	326787	302186
No. of unique reflections	37500	36782	35359
Completeness (%)	97.0 (83.9)	95.2 (73.1)	91.3 (44.6)
Multiplicity	8.9 (3.7)	8.9 (3.3)	8.5 (2.2)
Averaged $I/\sigma(I)$	7.4 (2.7)	6.9 (2.4)	6.4 (2.6)
$R_{\rm meas}$†	0.093 (0.319)	0.100 (0.353)	0.104 (0.355)
$R_{\rm ano}$‡	0.056 (0.196)	0.050 (0.230)	0.055 (0.262)
$R_{\rm ano}$ (relative scaling)‡	0.043 (0.163)	0.040 (0.193)	0.043 (0.254)
$R_{{\rm merge}\lambda}$§	0.075 (0.271)	0.074 (0.362)	—
$R_{{\rm merge}\lambda}$ (relative scaling)§	0.050 (0.171)	0.047 (0.160)	—

† $R_{\rm meas} = \sum_{hkl}[m/(m-1)]^{1/2}\sum_i |I_i(hkl) - \langle I(hkl)\rangle|/\sum_{hkl}\sum_i |I_i(hkl)|$, where $\langle I\rangle$ is the mean intensity of a set of equivalent reflections and m is the multiplicity of the data set. ‡ $R_{\rm ano} = \sum_{hkl} |\langle I(hkl)\rangle - \langle I(\overline{hkl})\rangle|/\sum_{hkl} |\langle I(hkl)\rangle + \langle I(\overline{hkl})\rangle|$. § $R_{{\rm merge}\lambda} = \sum_{hkl} |F_{\lambda i}(hkl) - F_{\lambda o}(hkl)|/\sum_{hkl} |F_{\lambda o}|$, where λ_o is the remote wavelength.

such as pH, temperature and protein concentration, the best single crystal of monomeric IDH was obtained at 291 K under the following conditions: reservoir solution consisting of 0.1 *M* HEPES–NaOH pH 7.0, 24.0%(*w*/*v*) PEG 6000, 20.0%(*v*/*v*) glycerol, 4.0 m*M* $MnCl_2$ and 4.0 m*M* DL-isocitrate and protein solution made up to a concentration of 8.0 mg ml^{-1} in 0.1 *M* HEPES–NaOH pH 7.0 and 10.0%(*v*/*v*) glycerol. Hanging drops were formed from 2.5 µl of a protein solution and 2.5 µl of a reservoir solution. Fig. 1 shows the improvement in crystal quality of monomeric IDH.

The X-ray absorption spectrum for the Mn *K* edge (Fig. 2) was measured using poor-quality polycrystals. Based on this fluorescence spectrum, two energies were chosen near the absorption edge of the Mn atom: 6.5516 keV (λ = 1.8923 Å) and 6.5478 keV (λ = 1.8934 Å). The third energy was selected at 6.6005 keV (λ = 1.8783 Å) as remote point. The crystal diffracted to a resolution of 2.9 Å. The crystal was found to belong to the orthorhombic system, space group $P2_12_12_1$, with unit-cell parameters a = 108.4, b = 121.7, c = 129.7 Å. The asymmetric unit contains two molecules of monomeric IDH, corresponding to a $V_{\rm M}$ value of 2.66 Å^3 Da^{-1} and a solvent content of 53.4% (Matthews, 1968). The crystallographic data and processing statistics are given in Table 1.

The absorption effect becomes a serious problem in the case of longer wavelengths near the Mn *K* edge being used to collect the diffraction data. The absorbed X-rays subsequently causes a thermal heating of and radiation damage to the crystal. The significant reduction of completeness in the order peak, edge and remote (Table 1) indicates a rather large degree of radiation damage in this experiment. The data scaled at each wavelength individually did not show Mn sites clearly in Bijvoet and dispersive difference Patterson maps (data not shown). Therefore, the diffraction data collected at different wavelengths were scaled to a reference data set that was calculated from all three data sets (relative scaling; Collaborative Computational Project, Number 4, 1994). This procedure also included smooth scaling across the detector (three-dimensional scaling), which partly corrected the absorption effect. Consequently both Bijvoet and dispersive difference Patterson maps showed two Mn sites in the asymmetric unit at 2.9 Å resolution very clearly. Harker sections of the Bijvoet difference Patterson map of peak data are given in Fig. 3. The coordinates of the two Mn sites [(0.99, 0.33, 0.31) and (0.49, 0.13, 0.19)] were determined with *SHELX*97 (Sheldrick, 1997) and *SOLVE* (Terwilliger &

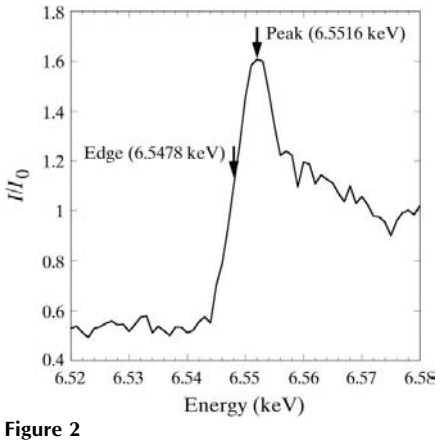

Figure 2
X-ray absorption plot for the Mn *K* edge. The absorption spectrum was measured on a beamline BL41XU at SPring-8.

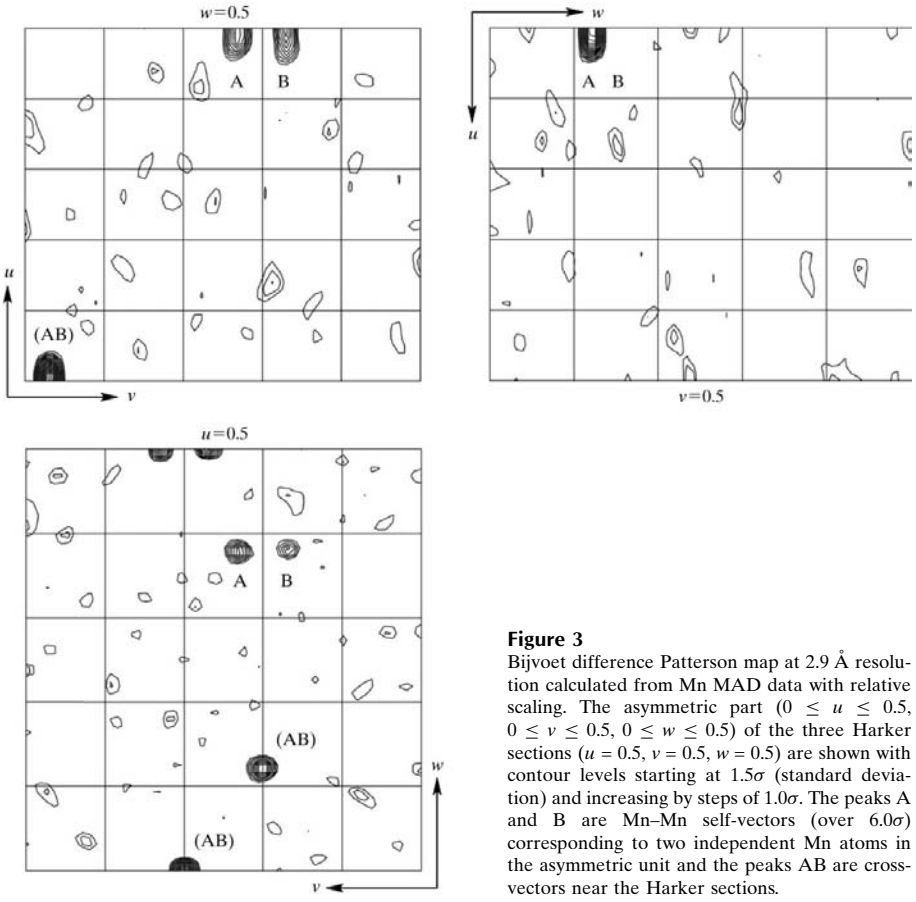

Figure 3
Bijvoet difference Patterson map at 2.9 Å resolution calculated from Mn MAD data with relative scaling. The asymmetric part ($0 \le u \le 0.5$, $0 \le v \le 0.5$, $0 \le w \le 0.5$) of the three Harker sections (u = 0.5, v = 0.5, w = 0.5) are shown with contour levels starting at 1.5σ (standard deviation) and increasing by steps of 1.0σ. The peaks A and B are Mn–Mn self-vectors (over 6.0σ) corresponding to two independent Mn atoms in the asymmetric unit and the peaks AB are cross-vectors near the Harker sections.

Berendzen, 1999). The heavy-atom parameters were refined and the initial phase was calculated with *SHARP* (La Fortelle & Bricogne, 1997). The molecular boundary in an asymmetric unit was determined unambiguously after the map improvement by solvent flipping; non-crystallographic symmetry (NCS) has already been defined.

We would like to thank Dr Kawamoto of the Japan Synchrotron Radiation Research Institute (JASRI) for his kind help in data collection. This work was supported in part by the 'Research for the Future' program (JSPS-RFTF 97L00501) of the Japan Society for the Promotion of Science.

References

Chen, R. D. & Gadal, P. (1990). *Plant Physiol. Biochem.* **28**, 411–427.
Cherbavaz, D. B., Lee, M. E., Stroud, R. M. & Koshland, D. E. Jr (2000). *J. Mol. Biol.* **295**, 377–385.
Collaborative Computational Project, Number 4 (1994). *Acta Cryst.* D**50**, 760–763.
Helliwell, J. R. (1992). *Macromolecular Crystallography with Synchrotron Radiation*, pp. 255–272. Cambridge University Press.
Hendrickson, W. H. (1991). *Science*, **254**, 51–58.
Hurley, J. H., Chen, R. & Dean, A. M. (1996). *Biochemistry*, **35**, 5670–5678.
Hurley, J. H., Dean, A. M., Koshland, D. E. Jr & Stroud, R. M. (1991). *Biochemistry*, **30**, 8671–8678.
Hurley, J. H., Dean, A. M., Sohl, J. M., Koshland, D. E. Jr & Stroud, R. M. (1990). *Science*, **249**, 1012–1016.
Hurley, J. H., Thorsness, P. E., Ramalingam, V., Helmers, N. H., Koshland, D. E. Jr & Stroud, R. M. (1989). *Proc. Natl Acad. Sci. USA*, **86**, 8635–8639.
Ishii, A., Suzuki, M., Sahara, T., Takada, Y., Sasaki, S. & Fukunaga, N. (1993). *J. Bacteriol.* **175**, 6873–6880.
La Fortelle, E. de & Bricogne, G. (1997). *Methods Enzymol.* **276**, 472–494.
Leslie, A. G. W. (1993). *Proceeedings of the CCP4 Study Weekend. Data Collection and Processing*, edited by L. Sawyer, N. Isaacs & S. Bailey, pp. 44–51. Warrington: Daresbury Laboratory.
Matthews, B. W. (1968). *J. Mol. Biol.* **33**, 491–497.
Rossmann, M. G., Moras, D. & Olsen, K. W. (1974). *Nature (London)*, **250**, 194–199.
Sheldrick, G. M. (1997). *Methods Enzymol.* **276**, 319–343.
Terwilliger, T. C. & Berendzen, J. (1999). *Acta Cryst.* D**55**, 849–861.